Raman spectroscopic investigation of speciation in $MgSO_4$(aq)

W. W. Rudolph[1,3*], G. Irmer[2], and G. T. Hefter[3*]

1) Medizinische Fakultät der TU Dresden, Institut für Virologie im MTZ, Fiedlerstr. 42 D-01307 Dresden, Germany
2) Institut für Theoretische Physik der TU Bergakademie Freiberg, Bernhard v. Cotta Str. 5, D- 09596 Freiberg, Germany
3) Chemistry Department, Murdoch University, Murdoch, WA 6150, Australia

* Corresponding authors

Abstract

Careful measurements have been made of the Raman spectra of aqueous solutions of $Mg(ClO_4)_2$, $MgCl_2$, $(NH_4)_2SO_4$ and $MgSO_4$ down to 50 cm^{-1} and, in some cases, to extremely low concentrations (≥0.0006 mol/kg) and high temperatures (≤200 °C). In $MgSO_4$(aq), the well known asymmetry in the ν_1-SO_4^{2-} mode at ~980 cm^{-1} that develops with increasing concentration has been assigned to a mode at 993 cm^{-1} associated with the formation of an $MgOSO_3$ contact ion pair (CIP). Confirmation of this assignment is provided by the simultaneous and quantitative appearance of stretching modes for Mg–OSO_3 of the ligated SO_4^{2-} at 245 cm^{-1} and for the $(H_2O)_5MgOSO_3$ unit at 328 cm^{-1}. The CIP becomes the dominant species at higher temperatures. Alternative explanations of the broadening of the ν_1-SO_4^{2-} mode are shown to be inconsistent with this and other Raman spectral evidence such as the similarity of the ν_1-SO_4^{2-} mode for $MgSO_4$ in H_2O and D_2O. After subtraction of the CIP component at 993 cm^{-1}, the ν_1-SO_4^{2-} band in $MgSO_4$(aq) showed systematic differences from that in $(NH_4)_2SO_4$(aq). This is consistent with a previously undetected ν_1-SO_4^{2-} mode at 982.2 cm^{-1} that can be assigned to the presence of solvent-shared ion pairs (SIPs). In solutions with high Mg^{2+}/SO_4^{2-} concentration ratios, a further ν_1-SO_4^{2-} mode was observed at

1005 cm^{-1}, which has been tentatively assigned to a $Mg_2SO_4^{2+}(aq)$ triple ion. All of these observations are shown to be in excellent agreement with recent dielectric relaxation spectroscopy measurements. In addition, the correct relationship between the Mg^{2+}/SO_4^{2-} association constant determined by Raman spectroscopic measurements and those obtained by other techniques is derived. It is shown that thermodynamic data measured by Raman spectroscopy for systems involving other (undetected) ion-pair types in addition to CIPs, cannot and should not be compared directly with those obtained by traditional techniques.

1. Introduction

Aqueous solutions of magnesium sulfate are of considerable practical importance as $MgSO_4$ has significant biological functions [1] and is a major component of seawater, where it is responsible for the high absorption of sound [2,3]. Magnesium sulfate is also present in many natural brines [4,5] and may occur at very high concentrations in environmental aerosols [6].

Not surprisingly therefore, $MgSO_4$(aq) solutions have been intensively investigated over a long period of time. Nevertheless, the speciation in this apparently simple system remains surprisingly poorly defined. Of the many techniques employed in the study of $MgSO_4$(aq), Raman spectroscopy has undoubtedly been one of the most useful and a number of such investigations have appeared [7-11]. Yet many of the features of the Raman spectra of $MgSO_4$(aq), such as the weak SO_4^{2-} bending modes and the low frequency Mg–O vibrations, remain poorly characterized. Even the interpretation of well-established spectral features, such as the developing asymmetry of the strong ν_1-SO_4^{2-} band at ~980 cm^{-1} with increasing $MgSO_4$ concentration, and their relationship to the speciation in $MgSO_4$(aq), has remained highly controversial [7,9-11].

A recent dielectric relaxation spectroscopy (DRS) study, performed over a wide range of concentrations and frequencies, has confirmed that $MgSO_4$(aq) is significantly associated[12]. More importantly, that study demonstrated unequivocally, as has long been inferred from ultrasonic absorption (UA) measurements,[13-15] that all three types of ion pair: double solvent-separated (2SIP), solvent-shared (SIP) and contact (CIP), co-exist in such solutions.

In view of the availability of these DRS results[12] and the steady improvements in Raman spectrometers in recent years[16,17] it is timely to make a detailed reinvestigation of the Raman spectra of $MgSO_4$(aq). However, to properly interpret such spectra it is essential to first thoroughly characterize the spectra of free (unassociated) Mg^{2+}(aq) and SO_4^{2-}(aq) ions. This paper therefore presents a detailed analysis of the spectra of $MgSO_4$(aq) and also of aqueous solutions of other relevant salts: $Mg(ClO_4)_2$, $MgCl_2$ and $(NH_4)_2SO_4$ and some of their mixtures. In addition, the relationship between the apparent association constant for $MgSO_4^0$(aq) obtained by Raman spectroscopy and those measured by other techniques is discussed in detail.

2. Experimental details and data analysis

2.1 Solution preparation

All solutions were prepared by weight, unless otherwise specified, from double glass-distilled water and the appropriate salt. Solution densities were measured with a pycnometer (5 mL) at 23 °C. Magnesium concentrations were determined by complexometric titration against standard EDTA [18].

A 2.213 mol/kg stock solution (pH = 6.26) of magnesium perchlorate was prepared from $Mg(ClO_4)_2 \cdot 6H_2O$ (Alfa Aesar, USA, reagent grade). The corresponding deuterated solution was prepared by dissolving $Mg(ClO_4)_2 \cdot 6H_2O$ in D_2O (Cambridge Isotope Laboratories, UK, 99.9 %). After several partial evaporations, the deuteration level, as determined by Raman spectroscopy, was found to be better than 99.0 %. Three magnesium chloride stock solutions (5.90; 3.48 and 3.30 mol/kg) were prepared from $MgCl_2 \cdot 6H_2O$ (Merck, p.a.). A 3.013 mol kg^{-1} magnesium sulfate stock solution (pH = 5.95) was prepared from $MgSO_4 \cdot 7H_2O$ (Merck, p.a.). A deuterated 2.093 mol/kg stock solution was formed by dissolving $MgSO_4 \cdot 7H_2O$ in D_2O. The deuteration level (Raman) after repetitive evaporation was better than 96.0 %. Ammonium sulfate stock solutions were prepared from $(NH_4)_2SO_4$ (Merck, p.a.). Stock solutions required for the determination of the scattering coefficient of ν_1-MgO_6 were prepared from $MgCl_2 \cdot 6H_2O$ and NH_4ClO_4 with the following concentrations (all mol/L): (2.336 $MgCl_2$ + 0.2738 NH_4ClO_4); 2.487 $MgCl_2$ + 0.1257 NH_4ClO_4);(2.888 $MgCl_2$ + 0.2478 NH_4ClO_4).

2.2 Raman spectroscopic measurements

All solutions were filtered through a 0.22 μm Millipore filter into 150 mm i.d. quartz tubes (~1 mL in volume) for Raman measurements. Raman spectra at higher temperatures and a few at room temperature were obtained with a Coderg PHO Raman spectrometer using the 488.0 nm argon ion laser line with a power level at the sample of about 900 mW as described elsewhere[17]. All other Raman measurements were performed at Freiberg using a triple-stage Jobin Yvon monochromator T64000 equipped with a liquid-nitrogen-cooled CCD detector. The spectra were recorded using a 90° scattering arrangement with the 514.5 nm

line of an Ar^+ -laser at a power level of 800 mW. The spectral resolution was normally 2.0 cm^{-1}. However, for the much narrower ν_1 mode of SO_4^{2-}, measurements were carried out in the additive mode with a spectral resolution of 0.7 cm^{-1}. $I_{||}$ and $I_\perp$ spectra were obtained with fixed polarisation of the laser beam by rotating the polarisator at 90 ° between the sample and the entrance slit to give the scattering geometries:

$$I_{||} = I(Y[ZZ]X) = 45\alpha'^2 + 4\gamma'^2 \quad (1)$$

$$I_\perp = I(Y[ZY]X) = 3\gamma'^2 \quad (2)$$

A program was applied that corrected the measured intensity for the fourth power frequency factor and then set the lowest data point to zero and the highest to 999 on a relative scale. This form of data is defined as the $I(\bar{\nu})$ spectrum and should be independent of the excitation frequency. The same program was applied to correct for the fourth power scattering factor, the Bose-Einstein temperature factor, $B = [1-\exp(-h\bar{\nu}\, c/kT]$ and the frequency factor, $\bar{\nu}$, to give the reduced or $R_Q(\bar{\nu})$ spectrum, which is directly proportional to the point-by-point relative scattering activity, $S_Q(\bar{\nu})$, in terms of mass-weighted normal coordinates, Q, in the double harmonic approximation. $R_Q(\bar{\nu})$ is the form of the Raman spectrum that most closely approaches the vibrational density of states [19]. The relationship between the $I(\bar{\nu})$ and $R_Q(\bar{\nu})$ forms of the spectra is given by eq. (3).

$$S_Q(\bar{\nu}) \propto R_Q(\bar{\nu}) = I(\bar{\nu}) \cdot \bar{\nu} \cdot B \quad (3)$$

The normalized isotropic R-spectra were constructed by subtraction:

$$R(\bar{\nu})_{iso} = R(\bar{\nu})_{||} - 4/3R(\bar{\nu})_\perp \quad (4)$$

In the low wavenumber region only the $I(\bar{\nu})$ and $R_Q(\bar{\nu})$ spectra are significantly different and only the R-format spectra are presented. It should be noted that one of the advantages of using isotropic spectra is that the baseline is almost flat in the wavenumber region of about 320 – 700 cm^{-1} allowing relatively unperturbed observation of any weak modes present.

For quantitative measurements, the perchlorate band, ν_1-ClO_4^- at 935 cm^{-1} was used as an internal standard. The relative isotropic scattering coefficient S(ν_1-MgO_6) was obtained from the R_{iso} spectra. The advantage of S values over J values is that S values can be put on an absolute scale[17]. Further details about the high temperature measurements, the band fitting procedure and R-normalized spectra are described elsewhere[17,20].

3. Results and Discussion

3.1 Characterization of unassociated $Mg(OH_2)_6^{2+}(aq)$

It is generally accepted that, although there may be minor levels of association in aqueous $Mg(ClO_4)_2$, and $MgCl_2$ solutions, in neither case does the anion penetrate into the first coordination sphere of the hexaquamagnesium(II) ion. That is, if any association does occur in such solutions only (weak) outer sphere complexes are formed. Such solutions are therefore appropriate for characterizing the spectral features of $Mg(OH_2)_6^{2+}(aq)$.

The isolated $Mg(OH_2)_6^{2+}$ species possesses T_h symmetry[20,21] so, with its 19 atoms, 3N – 6 = 51 nmv (normal modes of vibration) are expected and the irreducible representation is: $\Gamma_{vib}(T_h) = 3a_g + a_u + 3e_g + e_u + 5f_g + 8f_u$. The Raman active modes are a_g (totally polarized) and e_g and f_g (both depolarized). The nmv of $Mg(OH_2)_6^{2+}$ in the gas phase have been calculated by Pye and Rudolph [20] using *ab initio* methods. In aqueous solution, where the water modes can be considered as decoupled, it is sufficient to consider $Mg(OH_2)_6^{2+}$ as an MgO_6 unit of O_h symmetry with the water molecules being seen as point masses. The 51 nmv of $Mg(OH_2)_6^{2+}$ may then be divided into $6 \times 3 = 18$ internal and $6 \times 3 = 18$ external vibrations of the six coordinated water molecules and 15 modes of the MgO_6 unit [23]. The internal modes of the coordinated water molecules include deformation and stretching (at 1650 cm^{-1} and 3000 to 3500 cm^{-1}) whilst the external modes are librations (which are weak and broad at around 300 to 800 cm^{-1} [23]). These water modes are outside the scope of this paper and will not be discussed further.

The 15 nmv of the MgO_6 unit span the representation: $\Gamma_{vib}(O_h) = a_{1g} + e_g + 2f_{1u} + f_{2g} + f_{2u}$. The modes $\nu_1(a_{1g})$ (polarized), $\nu_2(e_g)$ and $\nu_5(f_{2g})$ (both depolarized) are Raman active whilst the $\nu_3(f_{1u})$ and $\nu_4(f_{1u})$ modes are IR active and the $\nu_6(f_{2u})$ mode is not active. The following

assignments of the various modes of MgO_6 are based on *ab initio* molecular orbital calculations for $Mg(OH_2)_6^{2+}$ and $Mg(OH_2)_6(OH_2)_{12}^{2+}$[11] which, for convenience, are summarized in Table 1.

The isotropic band at 358 cm^{-1} in the Raman spectrum (Figure 1**)** of $Mg(OH_2)_6^{2+}(aq)$**,** is assigned to the MgO_6 symmetric stretching mode $\nu_1(a_{1g})$. The Raman active $\nu_2(e_g)$ mode is too weak to be observed in solution spectra but can be seen at 315 ± 2 cm^{-1} in the Raman spectrum of $MgSO_4{\cdot}7H_2O$(cr)[23]. The broad depolarized mode at 235 cm^{-1} can be assigned to $\nu_5(f_{2g})$. In the IR spectrum, $\nu_3(f_{1u})$ has been observed at 420 cm^{-1}[11,22,23]. The clear differences in the positions of the Raman and IR bands support the assignment of O_h symmetry to MgO_6. In $MgCl_2/D_2O$ solutions, ν_1-$Mg(OD_2)_6^{2+}$ shifts to 342 cm^{-1}, which is in reasonable agreement with the expected isotope shift: ν_1-$Mg(OD_2)_6^{2+} = \sqrt{18.02/20.03} \times (\nu_1$-$Mg(OH_2)_6^{2+}) = 0.9485 \times 357\ cm^{-1} = 339\ cm^{-1}$.

With increasing temperature, the position of ν_1-MgO_6 in both $MgCl_2$(aq) and $Mg(ClO_4)_2$(aq) does not change significantly but broadens noticeably. For example, increasing the temperature of a 1.88 mol/kg $Mg(ClO_4)_2$) solution from 23 °C to 125 °C, shifted ν_1-MgO_6 from 358 cm^{-1} to 353 cm^{-1} whereas the full width at half height (fwhh) increased from 45 cm^{-1} to 58 cm^{-1}. Despite these changes the band symmetry was unaltered, confirming that neither ClO_4^- nor Cl^- penetrate into the inner-sphere of $Mg(OH_2)_6^{2+}$(aq)**.**

Relative intensity measurements for $MgCl_2$ solutions, using the R_{iso} spectrum with NH_4ClO_4 as an internal standard, yielded a corrected relative scattering coefficient[11] of $S_h = 0.0065 \pm 0.0005$ for the ν_1-MgO_6 mode, relative to $\nu_1(a_1)$-ClO_4^- at 935 cm^{-1}. This value is very small and reflects the fact that the electron density between Mg–O is not very high; in inorganic chemistry terms, the bond is mostly ionic. Much higher $S_h(\nu_1$-$MO_6)$ values are found for transition metal $M(OH_2)_6^{2+}$ ions: 0.032 for Zn [21], 0.045 for Cd [20] and 0.143 for Hg [20], reflecting an increase in softness (tendency to form covalent bonds) of the metal ions.

3.2 Characterization of unassociated SO_4^{2-}(aq)

The Raman spectral characteristics of the unassociated SO_4^{2-}(aq) ion can be established from measurements on $(NH_4)_2SO_4$(aq) solutions, which are generally thought to be fully dissociated. A recent *ab initio* molecular orbital study that included some Raman spectroscopic measurements of SO_4^{2-} hydration has been published by Pye and Rudolph [20]. The unassociated SO_4^{2-}(aq) ion has T_d symmetry and thus nine modes of internal vibration, having the representation: $\Gamma_{vib}(T_d) = a_1 + e + 2f_2$. All vibration modes are Raman active but only the f_2 modes are IR active.

The following features were observed for a 2.742 mol/kg $(NH_4)_2SO_4$ solution Raman spectrum (Figure 2). The $\nu_1(a_1)$-SO_4^{2-} mode centred on 979.5 cm^{-1} (fwhh = 6.95 ± 0.05 cm^{-1}) is almost totally polarised (ρ = 0.003, Figure 2B) whereas the $\nu_3(f_2)$-SO_4^{2-} band (not shown) centred on 1110 cm^{-1} (fwhh (R_{pol}) = 80 cm^{-1}) and the deformation modes $\nu_4(f_2)$-SO_4^{2-} at 617 cm^{-1} (fwhh (R_{pol}) = 42 cm^{-1}) and $\nu_2(e)$-SO_4^{2-} at 452 cm^{-1} (fwhh (R_{pol}) = 35 cm^{-1}) are depolarised. At low frequencies, a broad and very weak mode at ~190 cm^{-1} (fwhh ~170 cm^{-1}) is observed in the isotropic spectrum (Figure 2A). This mode is also observable in pure water and has been attributed to OH…O bonded water species.[23] In $(NH_4)_2SO_4$(aq) it may be assigned to the restricted translational mode of the OH…OSO_3^{2-} species. The corresponding bending mode of this unit is observable at ~60 cm^{-1}.[23]

The ν_1-SO_4^{2-} band shape is symmetrical in both polarisation arrangements but other band parameters vary slightly with concentration (Figures 3 and 4**)**. For example, at 23 °C for a 2.742 mol/kg $(NH_4)_2SO_4$ solution, ν_{max} shifted to slightly higher wavenumbers as the concentration is decreased, reaching 980.4 ± 0.1 cm^{-1} at infinite dilution (Figure 4A), whilst, using the narrow spectral slit width of 0.7 cm^{-1}, the fwhh decreased from (6.95 ± 0.05) cm^{-1} to (5.4 ± 0.1) cm^{-1} at infinite dilution (Figure 4B). Note that the signal-to-noise ratio for our spectra was excellent (≥500:1 even at 0.0184 mol/kg) and, for example, readily allowed the detection at 965 cm^{-1} of the ν_1-SO_4^{2-} mode of the isotopomer $S^{18}O^{16}O_3^{2-}$ (Figure 3 inset**)**, which has a natural abundance of only 0.80 mol%. More importantly for the present purposes, the symmetry of the ν_1- SO_4^{2-} mode was independent of the salt concentration over the entire range studied (Figure 3).

With increasing temperature the ν_1-SO_4^{2-} band shifted to lower frequencies and broadened.[17] For example, in a 3.780 mol/kg $(NH_4)_2SO_4$ solution ν_{max} varied smoothly from 979.4 ± 0.1 cm^{-1} at 23 °C to 977.0 ± 0.1 cm^{-1} at 200 °C whilst the fwhh increased from

7.10 ± 0.05 cm^{-1} to 11.0 ± 0.1 cm^{-1}.[17] Although the ν_1- SO_4^{2-} band shape remained symmetrical up to 200 °C it was not Lorentzian. Thus, at 23 °C the Gauss-Lorentz factor (R_{GL}) was 0.750 (i.e., there is a 25 % Gaussian contribution to the peak shape) but became more Lorentzian with increasing temperature (R_{GL} = 0.905 at 200 °C).[17] Similar behaviour was also found by Fujita and Kimura [23] who studied the relaxation of ν_1- SO_4^{2-} in aqueous Na_2SO_4 and $(NH_4)_2SO_4$ solutions at 5 – 80 °C.

3.3 Features of the Raman spectra of $MgSO_4$(aq)

The Raman spectra of aqueous solutions of $MgSO_4$ show many additional features to those of the unassociated SO_4^{2-}(aq) and $Mg(OH_2)_6^{2+}$(aq) modes described above. These are now discussed in detail.

3.3.1 Low frequency region (40 - 800 cm^{-1})

Significant differences exist between the Raman spectra of $(NH_4)_2SO_4$(aq) and $MgSO_4$(aq) in the low-frequency region. However, as has been explained above (and discussed in detail previously[16,17]), to make meaningful measurements in this region it is essential to use R-normalized data, so as to obtain spectra free of the influence of the broad quasi-elastic Rayleigh wing. Figure 5 compares the R_{II} spectrum of a 3.013 mol/kg $MgSO_4$ solution (middle trace) with that of a 3.780 mol/kg $(NH_4)_2SO_4$ solution (bottom trace) at 23 °C in the low wavenumber region. Both spectra exhibit the restricted translation mode of $OH\ldots OSO_3^{2-}$ at ~190 cm^{-1} along with the SO_4^{2-} deformation modes ν_2 at 452 cm^{-1} and ν_4 at 617 cm^{-1}. However, the latter two bands in $MgSO_4$(aq) are broadened relative to $(NH_4)_2SO_4$(aq) due to very weak contributions at 490 ± 10 cm^{-1} and 645 ± 5 cm^{-1}. Furthermore, in $MgSO_4$(aq) the ν_1-MgO_6 mode at 358 cm^{-1} develops a shoulder at 328 cm^{-1} and a new polarized mode at 245 cm^{-1} becomes apparent. All of these features become more pronounced with increasing temperature (Figure 5, top spectrum).

Details at low frequencies, including component decomposition, of the isotropic spectrum of the 3.013 mol/kg $MgSO_4$ solution are given in Figure 6. Whilst $Mg(ClO_4)_2$(aq) at 23 °C (Figure 1) shows only a symmetric ν_1-MgO_6 mode at 358 cm^{-1}, in $MgSO_4$(aq) the shoulder at ~328 cm^{-1} on the ν_1-MgO_6 mode is clearly distinguishable (Figure 6A). The most plausible

assignment of this component is that it is due to the Mg–OH_2 mode of the CIP [$(H_2O)_5MgOSO_3$], hereafter abbreviated ν_1-MgO_5O', for which further details are given below. The penetration of SO_4^{2-} into the first coordination sphere of the Mg^{2+} lowers the MgO_6 symmetry, which leads to a shift of the Mg–OH_2 symmetric stretch. No splitting is observed because the modes are too broad and overlap strongly. Even better evidence for direct contact between SO_4^{2-} and Mg^{2+} stems from the observation of the Mg^{2+}–OSO_3^{2-} vibration mode at 245 cm^{-1}. Consistent with increased formation of the CIP at higher temperatures (see Section 3.3.2 below), the component analysis shows that the relative importance of both the 328 and 245 cm^{-1} modes increases with increasing temperature (Figure 6B).

3.3.2 Sulfate stretching mode region (800 - 1300 cm^{-1})

The characteristics of the strong ν_1-SO_4^{2-} mode in $MgSO_4$(aq) differ considerably from those observed for the non-associated $(NH_4)_2SO_4$(aq) solutions (Figures 3, 4 and 7). As has been well established, [7,10,11] at ambient temperatures the ν_1-SO_4^{2-} mode at ~980 cm^{-1} shifts to higher wavenumbers and becomes increasingly asymmetric [24,25] as the $MgSO_4$ concentration rises (Figure 7). The changes in ν_{max} and the fwhh in $MgSO_4$(aq) are quantified and contrasted with those for $(NH_4)_2SO_4$(aq) in Figure 4.

Although there is general agreement about these observations[27], their interpretation has been controversial. Most authors[8,12,20] argue that they arise from CIP formation, which produces an additional ν_1-SO_4^{2-} mode at ~993 cm^{-1} (Figure 8A). Consistent with this assignment, the intensity of the 993 cm^{-1} mode decreases at lower concentrations and is virtually undetectable at ~0.0006 mol/kg (Figure 7). On the other hand, Nomura et al.[26, pp364-5] and later Rull et al. [27,28,29] have suggested that the changes in the ν_1-SO_4^{2-} mode are due to perturbations of the dynamics of water molecules around the sulfate ion.

This explanation can be refuted on many grounds. First, the 993 cm^{-1} band is present in the isotropic spectrum to which *only* vibrational relaxation processes contribute (i.e., there is no reorientational contribution to R_{iso} spectra)[30]. Second, as can be seen by comparing Figures 8A and 8B, there are no significant differences in the ν_1-SO_4^{2-} profile, including the contribution from the 993 cm^{-1} mode, for solutions of $MgSO_4$ in H_2O and D_2O. This would

be most unlikely if the ν_1-SO_4^{2-} mode contained an appreciable contribution from the solvent molecules. Third, DRS, which is particularly sensitive to variations in water molecule dynamics, detects no such changes[12]. Fourth, such effects would be expected to occur in all sulfate-containing electrolytes but they are absent from the Raman spectra of unassociated salts such as $(NH_4)_2SO_4$(aq) (Figures 3 and 4) and from salts such as Na_2SO_4(aq)[20] that are associated but that form only 2SIPs &/or SIPs.[31]

In another paper, Rull et al.[10] recognised the presence of the 993 cm^{-1} mode but associated it with some type of SIP. This assignment was based on two considerations. The first was that they did not observe the required changes in the Mg–O stretching mode or in the weak low frequency ν_2- and ν_4-SO_4^{2-} bending modes.[10] The second was that their calculation of the stability constant of $MgSO_4^0$(aq) via the Bjerrum equation was higher than the observed value if a CIP was assumed. This interpretation, which has been given currency by several reviewers [29,32], is untenable for a number of reasons.

As shown in Section 3.3.1 above (and elsewhere [11]), although the ν_2- and ν_4-SO_4^{2-} modes do not split, they *do* show effects consistent with the entry of SO_4^{2-} into the coordination shell of Mg^{2+}(aq). Figure 9 plots the integrated intensity of the ν-MgO_5O' component at 328 cm^{-1} against that of the ν_1-SO_4^{2-} component at 993 cm^{-1}, in each case normalized with respect to the total envelope for that mode. As required for the assignment of these two bands to the formation of a CIP, there is an excellent correlation ($r^2 = 0.997$) between their normalized intensities. The existence of CIPs rather than SIPs as the "last stage of [the] multistage association process"[10] between Mg^{2+}(aq) and SO_4^{2-}(aq) is confirmed by the dramatic increase in the ν_1-SO_4^{2-} mode at 993 cm^{-1} with temperature (Figure 10). Thus the small asymmetry in the ν_1-SO_4^{2-} mode at 23 °C becomes a clearly defined shoulder at 75 °C and ultimately the dominant component at 198 °C. Such behaviour would not be expected for SIPs (or water dynamics effects for that matter) but is consistent with increased CIP formation resulting from the weakening of the ion hydration shells with increasing temperature.

It may be added that by assuming SIPs as the final stage of association, Rull et al.[10], who also accepted the presence (as detected by UA techniques[13-15]) of three equilibria in the overall association process, were forced to postulate the formation of a triple solvent-

separated ion pair as the first stage. Such a species has, to the best of our knowledge, never been identified by any technique in any electrolyte solution; even if it did form, it could hardly be meaningful in terms of its lifetime. More damaging for this hypothesis, however: a triple solvent-separated ion pair, which would have a very large dipole moment, should be readily detected by DRS but is not.[12]

In addition, the suggestion by Rull et al.[10] that the Bjerrum equation can be used to assess the formation of particular types of ion pairs is unrealistic. This simple electrostatic model is at best a crude approximation (at least one experienced author[33] has described association constants calculated via the Bjerrum equation as "fictitious", which is perhaps a little harsh). To consider just one aspect of the Bjerrum model: its use of the bulk dielectric constant (ε) for electrolyte solutions, where dielectric saturation of the solvent in the vicinity of the ions may lower ε to a small fraction of its bulk value, removes any quantitative meaning from the results so produced[34].

3.4 Quantitative analysis of contact ion pair formation in $MgSO_4$(aq)

Given, as shown above, that the 993 cm^{-1} component of the ν_1-SO_4^{2-} mode can be assigned to CIP formation, it is possible to use Raman spectroscopy to derive an association constant for this species. This has been done in several studies[7,8,10,20] with the results being in reasonable agreement with each other. Unfortunately, there has been widespread misunderstanding about the significance of the constant so obtained[29,35] and in particular its relationship to other association constants reported in the literature for the same system. It is appropriate therefore to consider this matter in some detail.

The association between Mg^{2+}(aq) and SO_4^{2-}(aq) ions is generally thought to occur via a three step process, often referred to as the Eigen mechanism[13-15], in which the strongly solvated ions combine initially to form a 2SIP or, in the language of inorganic chemistry, an outer-outer sphere complex. The two intervening water molecules are then lost successively, forming SIPs and ultimately CIPs (outer and inner sphere complexes respectively). This process is summarized in the following reaction scheme:

$$\underset{\text{free aquated ions}}{Mg^{2+}(aq) + SO_4^{2-}(aq)} \overset{K_1}{\leftrightarrow} \underset{\text{2SIP}}{Mg^{2+}(OH_2)_2SO_4^{2-}(aq)} \overset{K_2}{\leftrightarrow} \underset{\text{SIP}}{Mg^{2+}(OH_2)SO_4^{2-}(aq)} \overset{K_3}{\leftrightarrow} \underset{\text{CIP}}{Mg^{2+}SO_4^{2-}(aq)} \quad (5)$$

where K_i (i = 1 to 3) are the 'stepwise' constants for the designated equilibria.

The overall association constant, K_A, as measured by traditional techniques such as potentiometry or conductivity, corresponds to the equilibrium:

$$Mg^{2+}(aq) + SO_4^{2-}(aq) \leftrightarrow MgSO_4^0(aq) \quad (6)$$

where $MgSO_4^0(aq)$ refers to all forms of associated $\{Mg^{2+}, SO_4^{2-}\}$ species of 1:1 stoicheometry in aqueous solution (thermodynamics makes no distinction between dissolved species of identical stoicheometry but with differing levels of solvation[36]). It is readily shown, ignoring activity coefficient effects throughout, that K_A is related to the K_i values via:

$$K_A = K_1 + K_1K_2 + K_1K_2K_3 \quad (7)$$

The K_i values, determined for example by UA[13-15] and DRS[12], are in good agreement and give values of K_A that lie well within the spread of reliable results reported in the literature using traditional methods. The equilibrium constant for the association between $Mg^{2+}(aq)$ and $SO_4^{2-}(aq)$ measured by Raman spectroscopy differs from both K_A and K_i.

Following previous studies[7,10,20] and the description given above, it is assumed that the ν_1-SO_4^{2-} band consists of only two significant components: a 'free' $SO_4^{2-}(aq)$ mode at ~980 cm^{-1} and the CIP mode at ~993 cm^{-1} (Figure 8A). In other words, only CIPs are spectroscopically distinct, in which case it follows that the 'free' $SO_4^{2-}(aq)$ mode must include contributions from 2SIP and SIP in addition to that from $SO_4^{2-}(aq)$. That is, the constant measured by Raman spectroscopy, K_R, corresponds to the equilibrium:

$$Mg^{2+}(aq) + \text{'free' } SO_4^{2-}(aq) \leftrightarrow CIP(aq) \quad (8)$$

where 'free' sulfate, as detected by Raman spectroscopy, $[SO_4^{2-}]_R = [SO_4^{2-}] + [2SIP] + [SIP]$ and thus

$$K_R = \frac{[CIP]}{[Mg^{2+}][SO_4^{2-}]_R} \tag{9}$$

In practice, K_R is formulated in terms of α, the spectroscopically-determined fraction of sulfate present as CIPs:

$$\alpha = I_{993}/(I_{980} + I_{993}) = [CIP]/C_T \tag{10}$$

where C_T is the total (analytical) concentration of $MgSO_4$. From the equilibrium stoicheometry

$$K_R = \frac{\alpha}{(1-\alpha)^2 C_T} \tag{11}$$

and thus it follows that:

$$K_R = \frac{[CIP]}{(C_T - [CIP])^2} \tag{12}$$

From eq. (5) and the appropriate equilibrium constant expressions:

$$[CIP] = K_1K_2K_3[Mg^{2+}]\,[SO_4^{2-}] \tag{13}$$

Furthermore, in stoichiometric $MgSO_4$(aq) solutions, assuming only 1:1 species are formed, mass balance demands that:

$$C_T = [MgSO_4]_T = [Mg^{2+}]_T = [SO_4^{2-}]_T \tag{14}$$

and

$$[Mg^{2+}] = [SO_4^{2-}] \tag{15}$$

Combination of equations (12)-(15) then gives:

$$K_R = \frac{K_1 K_2 K_3 [Mg^{2+}]^2}{(C_T - K_1 K_2 K_3 [Mg^{2+}]^2)^2} \quad (16)$$

Combination of the mass balance expressions:

$$[Mg^{2+}]_T = [Mg^{2+}] + [2SIP] + [SIP] + [CIP] \quad (17)$$

$$[SO_4^{2-}]_T = [SO_4^{2-}] + [2SIP] + [SIP] + [CIP] \quad (18)$$

with eq. (7) gives a quadratic expression:

$$K_A[Mg^{2+}]^2 + [Mg^{2+}] + [Mg^{2+}]_T = 0 \quad (19)$$

that can be solved algebraically for $[Mg^{2+}]$. Substitution of the physically meaningful root of eq. (19) into eq. (16) enables calculation of K_R from the K_i values (and K_A). Together, eqs. (16) and (19) define the relationship between K_R and the stepwise constants (K_i) determined by UA or DRS, and the overall association constant (K_A) determined thermodynamically. It follows that direct comparison of K_R with K_A, as has often been made in the literature,[29, 35] is incorrect. Note too that, whilst K_R can be calculated from K_i (and K_A), neither K_i nor K_A can be obtained uniquely from a single measurement of K_R.

The equations derived here for the Mg^{2+}/SO_4^{2-} system are applicable to any system that involves the formation of, in addition to CIPs, significant amounts of 2SIPs &/or SIPs, and to any technique which, like Raman spectroscopy, detects only CIPs. Thus similar considerations will apply to most types of NMR and UV-vis spectroscopy. It also follows that other thermodynamic quantities such as ΔH and ΔS that can be derived from the temperature dependence of K_R[29] are not comparable with those obtained by conventional thermodynamic methods. To put the situation bluntly, equilibrium constants for CIPs derived from Raman spectroscopy in systems containing undetected 2SIPs and/or SIPs are technique-specific. Such constants are not comparable with those obtained by thermodynamic techniques and cannot for example be used in speciation calculations. For this reason no such parameters are derived from the present Raman data.

Regardless of the complicated relationship between K_R, K_A and K_i, it is noteworthy that both Raman spectroscopy and DRS detect CIPs directly, so it is possible to make a quantitative comparison between them. Figure 11 shows the present Raman results (expressed as the fraction of SO_4^{2-} present as CIPs: $\alpha = [CIP]/ [SO_4^{2-}]_T = I_{993}/ (I_{993} + I_{980})$ and noting that the scattering coefficients for bound and free sulphate are equal) as a function of $[MgSO_4]_T$ and compares them with those obtained by DRS[12]. Given the likely uncertainties in both sets of data the agreement is excellent and provides further evidence that the 993 cm^{-1} mode is indeed due to CIPs.

3.5 Detailed interpretation of the ν_1-SO_4^{2-} band shape

To quantify the degree of CIP formation in Section 3.4 it was assumed that the ν_1-SO_4^{2-} mode consisted of only two components: one at ~980 cm^{-1} associated with 'free' SO_4^{2-} and the other at ~993 cm^{-1} associated with CIPs. On this basis, and consistent with the generally accepted view that, when using only ligand vibrations, 2SIPs and SIPs are indistinguishable from the unassociated ion,[37] it would be expected that subtraction of the CIP contribution from the ν_1-SO_4^{2-} envelope would produce a mode with characteristics similar to those observed for ν_1-SO_4^{2-} in solutions of an unassociated salt such as $(NH_4)_2SO_4$. However, when this decomposition is performed, the 'free' SO_4^{2-} mode in $MgSO_4$(aq) shows systematic differences from that observed for $(NH_4)_2SO_4$(aq). In particular (Figure 4), the ν_1-SO_4^{2-} mode in $MgSO_4$(aq) at ~980 cm^{-1}, after removal of the 993 cm^{-1} component, shows changes in position and fwhh with increasing concentration that are of much greater magnitude and, in the case of ν_{max}, in the *opposite direction* to those of ν_1-SO_4^{2-} in $(NH_4)_2SO_4$(aq). These effects are small ($\Delta\nu_{max} \leq 2$ cm^{-1}; Δfwhh ≤ 2.5 cm^{-1}) but they are reproducible; similar changes have recently been reported using an FT Raman spectrometer[12]. Importantly, in very dilute solutions (Figures 3, 4 and 7) the shape and location of the ν_1-SO_4^{2-} mode in $MgSO_4$(aq) and $(NH_4)_2SO_4$(aq) become identical. These features, along with the very narrow slit widths employed and the quality of the present spectra, make it highly unlikely that these observations are artefactual.

In aqueous solution, the sulfate modes are influenced by the environment (environmental broadening). Whilst there is probably a continuum of perturbing environments, it can be assumed that there are preferred energy minima within this continuum. These minima can be

interpreted as corresponding to ion pairs. Thus, the most straightforward explanation for these effects is that the 'free' SO_4^{2-} mode at ~980 cm^{-1} overlaps with another mode centred at slightly higher wavenumbers. It seems both plausible and chemically reasonable to assign this extra mode to the presence of SIPs. Although (and as discussed above) it is generally thought [37] that Raman spectra involving anion vibrations can distinguish only between 'free' anions and those involved in direct bonding to cations (CIPs), James and Frost [38,39] have detected both CIPs and SIPs in their Raman studies of weak metal ion/nitrate complexes in aqueous solutions. Their assignment was based on a Fourier transform procedure for signal narrowing and subsequent band fitting, and assumed that the peak positions of the 'free' nitrate and the nitrate in the SIPs and CIPs were virtually independent of concentration. The other sulfate modes also show effects consistent with the formation of SIPs. Thus, the restricted O–H…OSO_3^{2-} stretching mode at ~190 cm^{-1} in 2 mol/L $MgSO_4$(aq)) is much broader (fwhh ≈ 205 cm^{-1}) than in 2 mol/L $(NH_4)_2SO_4$(aq) (fwhh ≈ 175 cm^{-1}) and ν_2- and ν_4-SO_4^{2-} in $MgSO_4$(aq) are broadened compared with $(NH_4)_2SO_4$ (aq) (Figure 5).

Although the above assignment appears reasonable, an unambiguous decomposition of the 'free' ν_1-SO_4^{2-} band (after subtraction of the 993 cm^{-1} mode) is difficult because of the close proximity of the components. The fitting procedure employed was based on considerations similar to those used by Frost and James [38,39]. As the effects of SIP formation on ν_1- SO_4^{2-} were very much less than those of CIP formation, it was assumed that 2SIPs would not be Raman-distinguishable from SO_4^{2-}(aq). The total ν_1-SO_4^{2-} mode was then fitted with the minimum number of components that produced concentration-independent band parameters, except for the intensity. The concentrations of CIPs, SIPs and {2SIP + SO_4^{2-}(aq)} derived from the present decomposition of the ν_1-SO_4^{2-} mode along with the corresponding values determined from DRS measurements are plotted in Figure 12. Given the number of species involved, the probable experimental errors, and the uncertainties with regard to the decomposition of the overlapping bands in both techniques, the level of agreement is very gratifying.

3.6 Spectra at high $[Mg^{2+}]_T/[SO_4^{2-}]_T$ ratios

Most Raman spectroscopy on the $\{Mg^{2+} + SO_4^{2-} + H_2O\}$ system has been made using solutions prepared directly from magnesium sulfate in which the Mg^{2+}/SO_4^{2-} concentration ratio is necessarily 1:1. Recently, qualitative evidence was obtained for an additional feature in the ν_1-SO_4^{2-} mode in solutions with very high $[Mg^{2+}]_T/[SO_4^{2-}]_T$ ratios[12]. Figure 13 shows the Raman spectrum in the ν_1-SO_4^{2-} region for a solution containing 0.0956 mol/L $MgSO_4$ and 3.670 mol/L $MgCl_2$ at 23 °C. Consistent with the previous findings[12] but much more easily discernible in the present higher quality spectra, an additional feature is clearly present at ~1005 cm^{-1}. Comparable results (not shown) were obtained under a variety of conditions and a similar feature has also been detected by FT Raman microscopy on highly supersaturated $MgSO_4$(aq) droplets [6,40]. The present results are insufficient to unambiguously assign this mode but, consistent with the DRS data[12], it can probably be assigned to the formation of a (contact) triple ion $Mg_2SO_4^{2+}$(aq) ('TI'), in which the SO_4^{2-} directly bonds to (i.e., bridges) two Mg^{2+} ions. Other possibilities include the formation of a bidentate CIP or larger Mg^{2+}, SO_4^{2-} clusters[6,40].

4. References and notes

1) Berthon, G., Ed. *Handbook of Metal-Ligand Interactions* ; Dekker : New York, 1995.
2) Fisher, F. H. *Science* **1967**, *157*, 823.
3) Fisher, F. H. *Geochim. Cosmochim. Acta*, **1972**, *36*, 99.
4) Riley, J. P.; Skirrow, G., *Chemical Oceanography*; Academic Press: London, 1975.
5) Gianguzza, A. Pelizetti, E.; Sammartano, S., Ed. *Chemistry of Marine Water and Sediments*, Sprinter: Berlin, 2002.
6) Zhang, Y.-H.; Chan, C. K., *J. Phys. Chem. A*, **2002**, *106*, 285.
7) Davis, A. R.; Oliver, B. G. *J. Phys. Chem*. **1973**, *77*, 1315.
8) Chatterjee, R. M.; Adams, W. A.; Davis, A. R. *J. Phys. Chem*. **1973**, *78*, 246.
9) Daly, F. P.; Brown, C.; Kester, D. R. *J. Phys. Chem*. **1973**, *76*, 3664.
10) Rull, F.; Balarew, Ch.; Alvarez, J. L.; Sobron, F.; Rodriguez, A. *J. Raman Spectrosc*. **1994,** *25*, 933.
11) Pye, C. C.; Rudolph, W. W. *J. Phys. Chem. A*, **1998**, *102*, 9933.
12) Buchner, R.; Chen, T.; Hefter, G. *J. Phys. Chem*. 2003, submitted.

13) Eigen, M.; Tamm, K. *Z. Elektrochem.* **1962**, *66*, 93.

14) Eigen, M.; Tamm, K. *Z. Elektrochem.* **1962**, *66*, 107.

15) Atkinson, G.; Petrucci, S. *J. Phys. Chem*. **1966**, *70*, 3122.

16) Rudolph, W. W.; Brooker, M. H.; Pye, C.C., *J. Phys. Chem*. **1995**, *99*, 3793.

17) Rudolph, W. W. *Z. Phys. Chem*. **1996**, *194*, 73.; Rudolph, W. W. ; Pye, C.C. ; Irmer, G. *J. Raman Spectrosc*. **2002**, *33*, 177.

18) Schwarzenbach, G. Flaschka, H., *Complexometric Titrations*, 2nd edition, Methuen, London, 1969.

19) Rudolph, W. W.; Irmer, G. *J. Solution Chem*., **1994**, *23*, 663; Rudolph, W. W.; Brooker, M. H.; Tremaine, P. R., *Z. Phys. Chem.*, **1999**, *209*, 181.

20) Pye, C. C.; Rudolph, W. W. *J. Phys. Chem. A*, **2001**, *105*, 905.

21) Rudolph, W. W.; Schoenherr, *Z. Phys. Chem*.(Leipzig), **1989,** *270*, 1121.

22) The value of 310 cm^{-1} reported for $\nu_3(f_{1u})$ in $MgSO_4 \cdot 7H_2O$(cr) by Nakagawa and Shimanouchi [23] is almost certainly incorrect. Careful inspection of the published IR spectrum[23] shows a weak mode at ~400 cm^{-1}.

23) Nakagawa, I.; Shimanouchi, T., *Spectrochim. Acta*, **1964**, *20*, 429; Fujita, K.; Kimura, M. *J. Raman Spectrosc*. **1981,** *11*, 108.

24) Earlier reports [9,25] of a symmetrical ν_1-SO_4^{2-} band in $MgSO_4$(aq) are incorrect. Such observations reflect the swamping of the relatively small asymmetry by band broadening due to the large (10 cm^{-1}) slit widths then commonly available.

25) Hester, R. E.; Plane, R. A., *Inorg. Chem.* 1964, *3*, 769.

26) Nomura, H.; Koda, S.; Miyahara, Y., in *Water and Cations in Biological Systems*, B. Pullman; K. Yagi eds. (Japan Scientific Soc., Tokyo, 1980) p. 31.

27) Rull, F.; Sobron, F., *J. Raman Spectrosc*. **1994,** *25*, 693.

28) Rull, F.; Ohtaki, H. , *Spectrochim Acta, A,* **1997,** *53*, 643.

29) Alia, J. M., *Handbook of Raman Spectroscopy*, Eds. Lewis, I. R.; Edwards, H. G. M., Marcel Dekker, New York, **2001**.

30) Griffiths, J. E., in : *Vibrational Spectra and Structure*, Vol.6, Ed. Durig, J. R.; Elsevier Amsterdam, **1977**.

31) Buchner, R.; Capewell, S. G.; Hefter, G. T.; May, P. M. *J. Phys. Chem. B* **1999**, *103*, 1185.

32) Myneni, S. C. B. *Rev. Mineral. Geochem.* **2000**, *40*, 113.

33) Malatesta, F., *Quim. Analit.*, **1996**, *15*, S9.

34) Conway, B. E. In *Modern Aspects of Electrochemistry*, Conway, B. E.; White, R. E. (eds); vol 35, Kluwer Academic/Plenum: New York, 2002, p295ff.

35) See for example, Rard, J. A. *J. Chem. Thermodyn.* **1997**, *29*, 533.

36) Hepler, L. G.; Hopkins, H. P. *Rev. Inorg. Chem.* **1979**, *1*, 333.

37) See for example, Brooker, M. H. Raman Spectroscopic Measurements of Ion Hydration. In *The Chemical Physics of Ion Hydration*; Dogonadze, R. R. et al., Eds.; Elsevier: Amsterdam, 1986; Part B, Ch.4.

38) James, D. W.; Frost, R. L., *Aust. J. Chem.*, **1982**, *35*, 1793.

39) James, D. W.; Carrick, M. T.; Frost, R. L., *J. Raman Spectrosc.*, **1982**, *13*, 115.

40) Zhang, Y.-H.; Chan, C. K. *J. Phys. Chem. A*, **2000**, *104*, 9191.

41) The R_{iso} profile of the ν_1-SO_4^{2-} mode has been taken from the R_{II} spectrum [33] because of the very low contribution from the anisotropic scattering. However, in aqueous solutions the water background has to be taken into account because ν_1-SO_4^{2-} is sitting on edge of the rocking mode of water (ca. 870 cm^{-1}). Use of the R_{iso} profile has the advantage that the scattering contribution of the water is partially removed.

Table 1. MgO_6 skeleton modes (O_h symmetry) of the $Mg(OH_2)_6^{2+}$ cation. Experimental wavenumbers and calculated wavenumbers (unscaled) in aqueous solution.

Assignment and activity of mode	Experimental[a] wavenumbers (cm^{-1})	Calculated[b] wavenumbers (cm^{-1})
$\nu_1(a_{1g})$, R	357.5 ± 0.5	356
$\nu_2(e_g)$, R	315 ± 2	334
$\nu_3(f_{1u})$, IR	420 ± 2	449
$\nu_4(f_{1u})$, IR	-	113
$\nu_5(f_{2g})$, R	240 ± 4	264
$\nu_6(f_{2u})$, n.a.	-	96

[a] Determined in $MgCl_2$(aq) and $Mg(ClO_4)_2$(aq), see text.
[b] Unscaled HF/6-31G(d) wavenumbers of MgO_6 unit of the octadecaaqua magnesium(II) (T symmetry); taken from Pye and Rudolph ref. 20.

Captions for Figures

1) Raman spectrum (R_{iso} format) of a 2.213 mol/kg $Mg(ClO_4)_2$ solution at 23 °C, showing the sum, component and (bottom trace) residual curves. The ν_1-MgO_6 mode of $Mg(OH_2)_6^{2+}$ is at 358 cm^{-1} and the broad OH…$OClO_3^-$ restricted translation mode is at ~235 cm^{-1}.

2) Raman spectrum (R format) of 2.742 mol/kg $(NH_4)_2SO_4$(aq) at 23 °C. A (50 to 700 cm^{-1}): ν_2 and ν_4 bending modes of SO_4^{2-} at 452 $cm^{-1}$and 617 cm^{-1}; OH…OSO_3^{2-} restricted translation mode at ~190 cm^{-1}. B (920 to 1040 cm^{-1}): ν_1-SO_4^{2-} mode (note $R_{iso} \approx R_{pol}$ for this totally polarized mode). The broad, weak ν_3-SO_4^{2-} mode at 1110 cm^{-1} [22] is omitted for clarity.

3) Concentration dependence of the ν_1-SO_4^{2-} Raman mode (R_{iso} format) of $(NH_4)_2SO_4$(aq) at 23 °C. Inset: spectrum of 0.233 mol/kg $(NH_4)_2SO_4$ showing the detection of the isotopomer $S^{18}O^{16}O_3^{2-}$ at 964 cm^{-1}.

4) Concentration effects at 23 °C on the ν_1-SO_4^{2-} mode at ~980 cm^{-1} in $(NH_4)_2SO_4$ solutions (filled circles) and in $MgSO_4$ solutions (after subtraction of the 993 cm^{-1} component, open circles); A: peak position (ν_{max}); B: fwhh.

5) Raman spectra (R_{pol} format) of $(NH_4)_2SO_4$(aq) at 23 °C and $MgSO_4$(aq) at 23 and 120 °C at low wavenumbers, showing the restricted OH…OSO_3^{2-} translation mode at ~190 cm^{-1}, the Mg^{2+}–OSO_3^{2-} mode at ~245 cm^{-1}, the MgO_6 stretching modes at ~328 and 358 cm^{-1}, and the SO_4^{2-} deformation modes, ν_2 and ν_4 at ~452 and 617 cm^{-1}.

6) Temperature effects on the R_{iso} spectrum at low frequencies of 3.013 mol/kg $MgSO_4$(aq), showing the sum curve and component modes at A: 23 °C; B: 120 °C. Note the increasing importance at 120 °C of the 326 cm^{-1} component of the ν_1-MgO_6 mode and of the Mg^{2+}–OSO_3^{2-} mode at 245 cm^{-1}.

7) Concentration dependence of the R_{iso} spectrum in the ν_1-SO_4^{2-} region for $MgSO_4$(aq) at 23 °C.

8) R_{iso} spectrum, showing the sum, component and (bottom trace) residual curves at 23 °C for A: 2.093 mol/kg $MgSO_4$ in H_2O; B: 2.106 mol/kg $MgSO_4$ in D_2O,. Note that the isotopomeric component is included in the fit but omitted for clarity.

9) Correlation between the normalized integrated band intensities $I_{328}/(I_{328} + I_{358})$ and $I_{993}/(I_{993} + I_{980})$ for four concentrations (2.848; 2.106; 1.365, and 0.681 mol/kg) of $MgSO_4$(aq) at 23 °C.

10) Effects of temperature on the ν_1-SO_4^{2-} mode (R_{iso} format) of 0.571 mol/kg $MgSO_4$(aq).

11) Fraction of sulfate species present as contact ion pairs as a function of $[MgSO_4]_T$, as determined by: Raman spectroscopy (present work, 23 °C, squares) and DRS (ref. 12, 25 °C, circles).

12) Comparison of the % species detected by Raman spectroscopy (upper panel) and by DRS (lower panel): filled triangles, 2SIP + SO_4^{2-}(aq); filled squares, SIP; filled stars, CIP + TI.

13) R_{iso} spectrum for a solution containing 4.098 mol/kg $MgCl_2$ + 0.107 mol/kg $MgSO_4$ at 23 °C, showing the sum, component and (bottom trace) residual curves. For clarity, only a single component was used to fit the 'free' SO_4^{2-} and the isotopomeric component (included in the fit) was omitted from the diagram. Note the appearance of the new mode at 1005 cm^{-1}, which has been assigned to a triple ion, $Mg_2SO_4^{2+}$(aq).

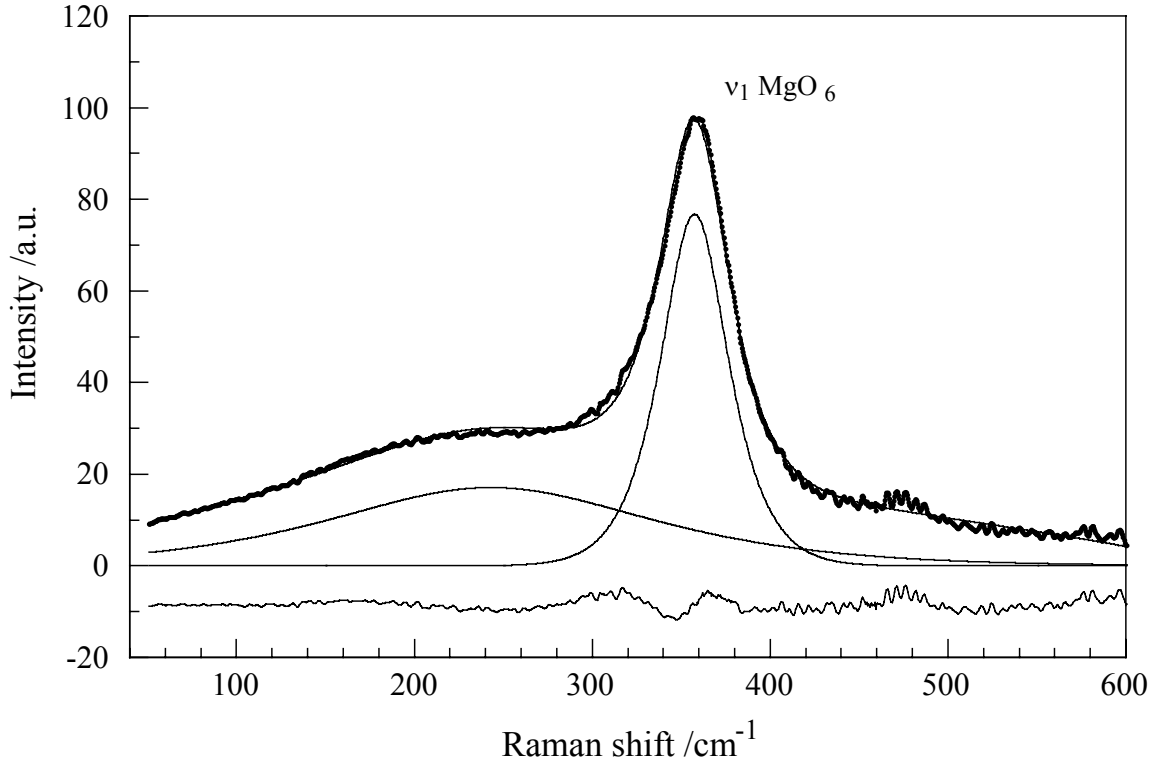
120
100
80
60
40
20
0
-20
Intensity /a.u.
100
200
300
400
500
600
Raman shift /cm-1
ν1 MgO 6

Figure 1

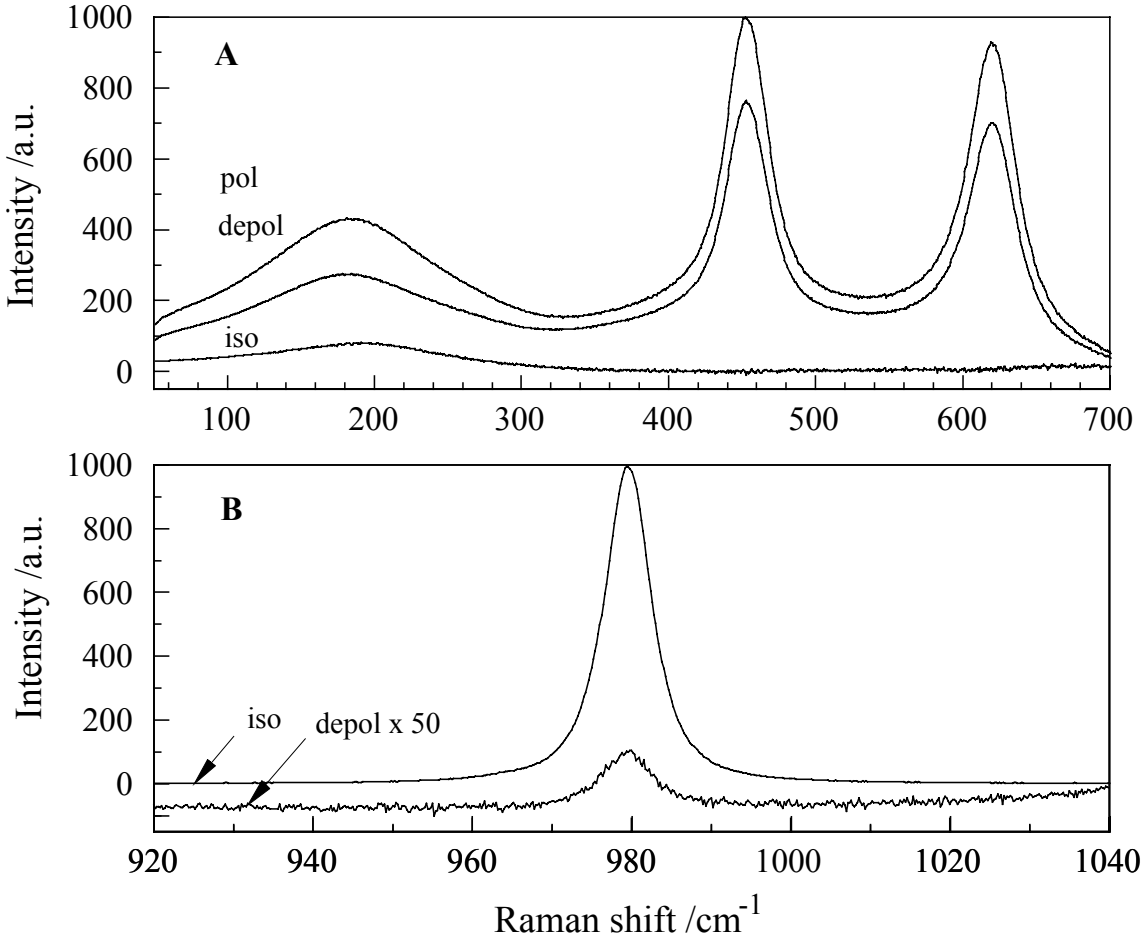
A
pol
depol
iso
Intensity /a.u.
1000
800
600
400
200
0
100
200
300
400
500
600
700
B
iso
depol x 50
Intensity /a.u.
920
940
960
980
1000
1020
1040
Raman shift /cm-1

Figure 2

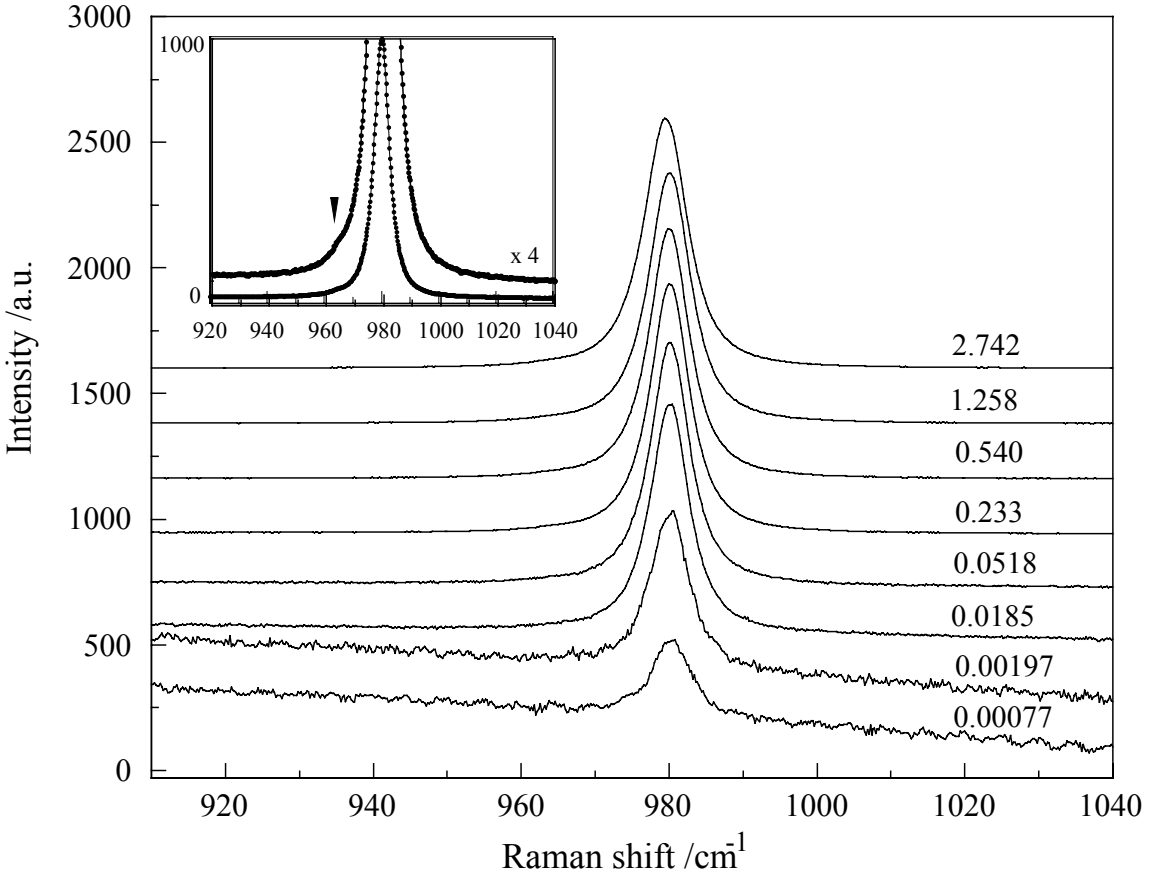
3000
2500
2000
1500
1000
500
0
Intensity /a.u.
920
940
960
980
1000
1020
1040
Raman shift /cm-1
1000
0
x 4
2.742
1.258
0.540
0.233
0.0518
0.0185
0.00197
0.00077

Figure 3

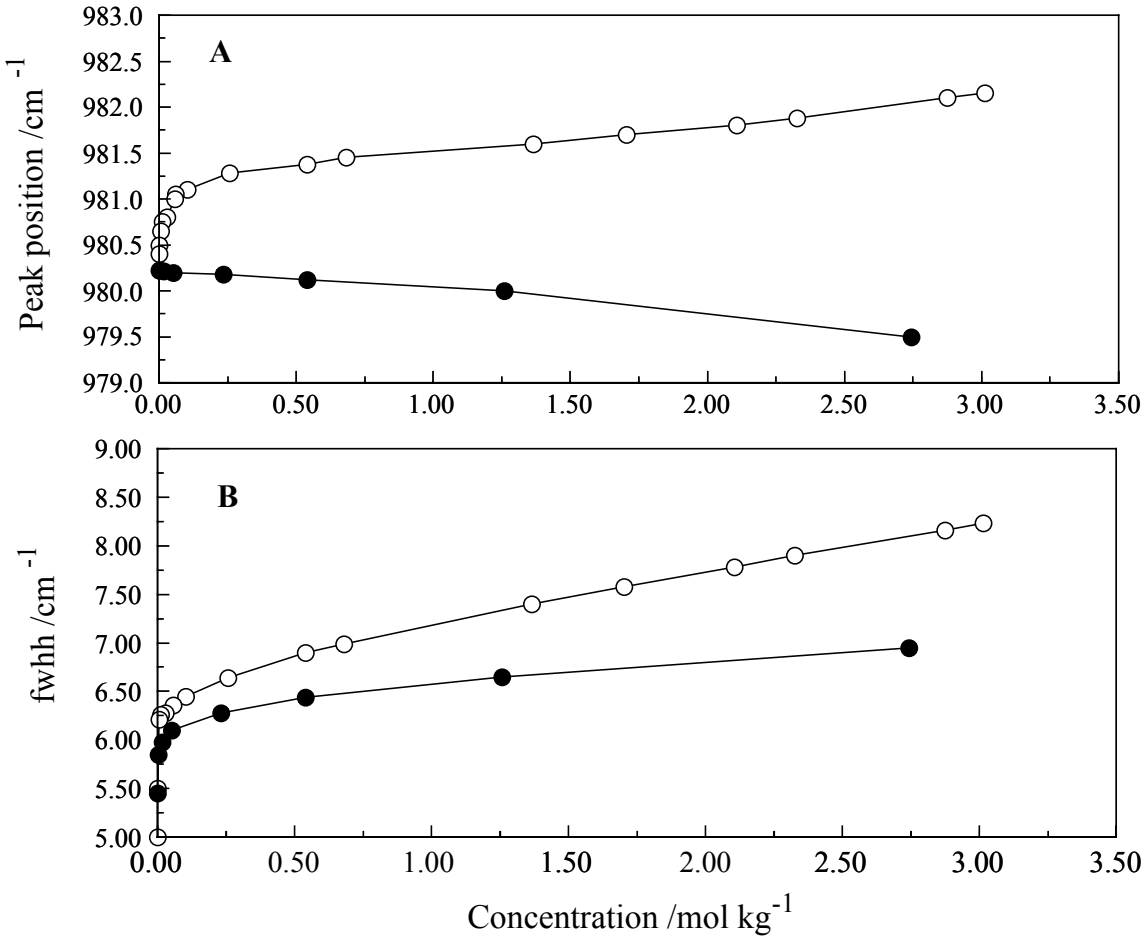
A
B
Peak position /cm -1
fwhh /cm -1
Concentration /mol kg-1
983.0
982.5
982.0
981.5
981.0
980.5
980.0
979.5
979.0
9.00
8.50
8.00
7.50
7.00
6.50
6.00
5.50
5.00
0.00
0.50
1.00
1.50
2.00
2.50
3.00
3.50

Figure 4

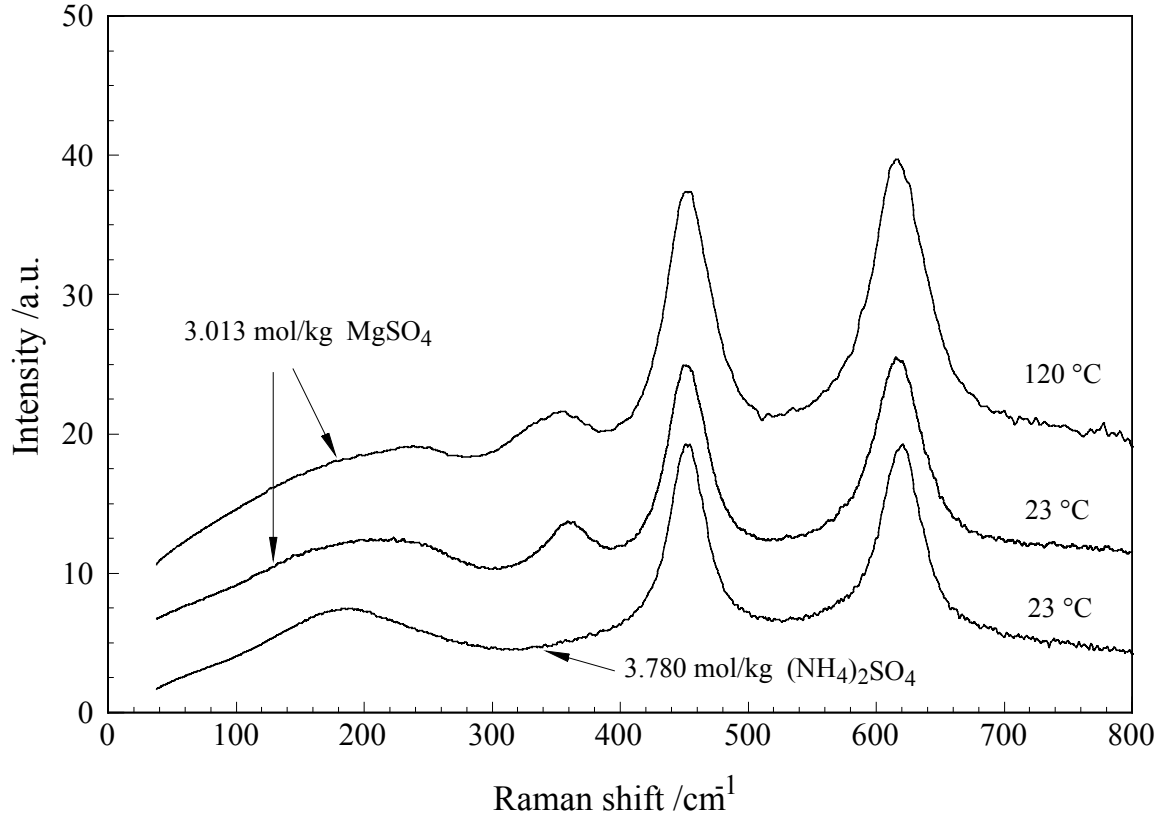
Intensity /a.u.
Raman shift /cm-1
3.013 mol/kg MgSO4
3.780 mol/kg (NH4)2SO4
120 °C
23 °C
23 °C
0
10
20
30
40
50
0
100
200
300
400
500
600
700
800

Figure 5

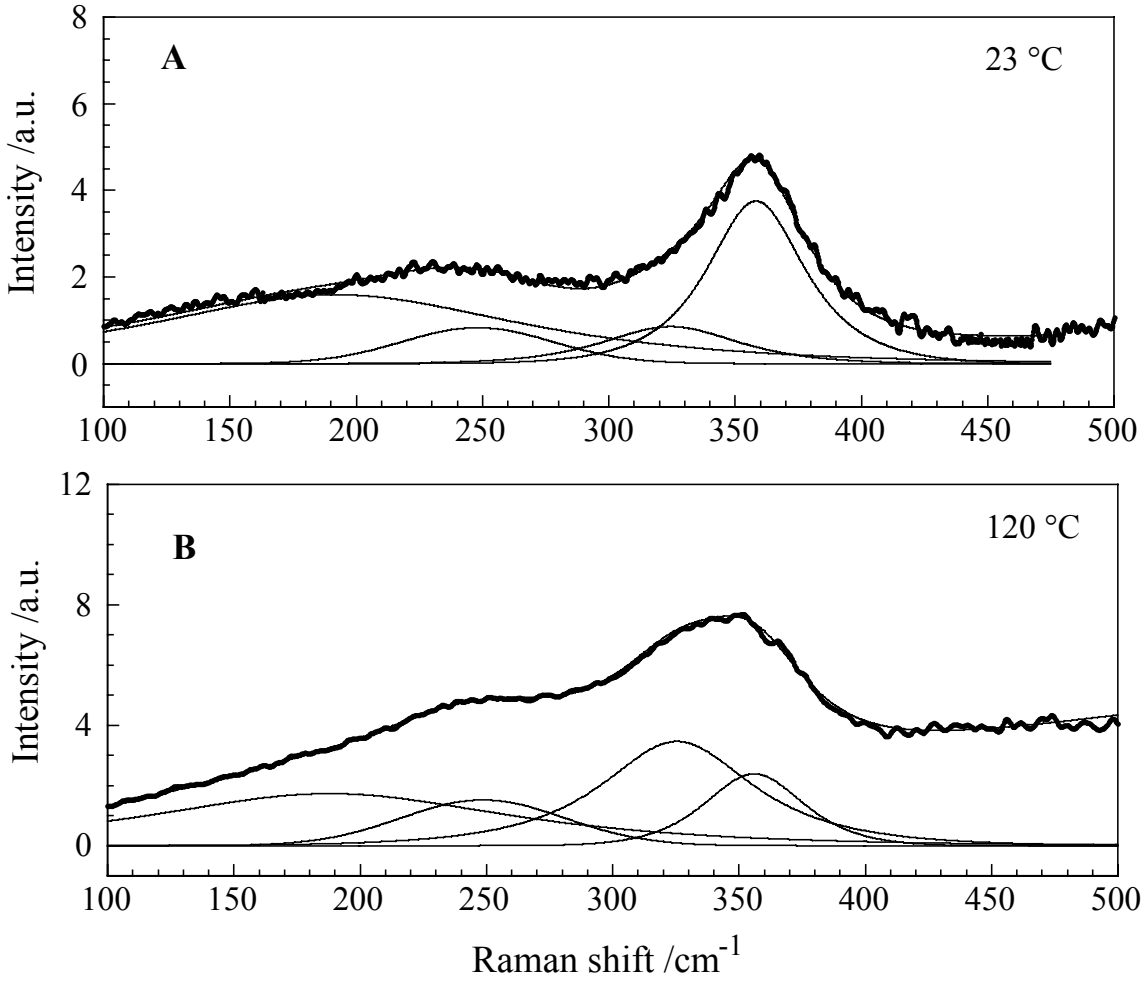

Figure 6

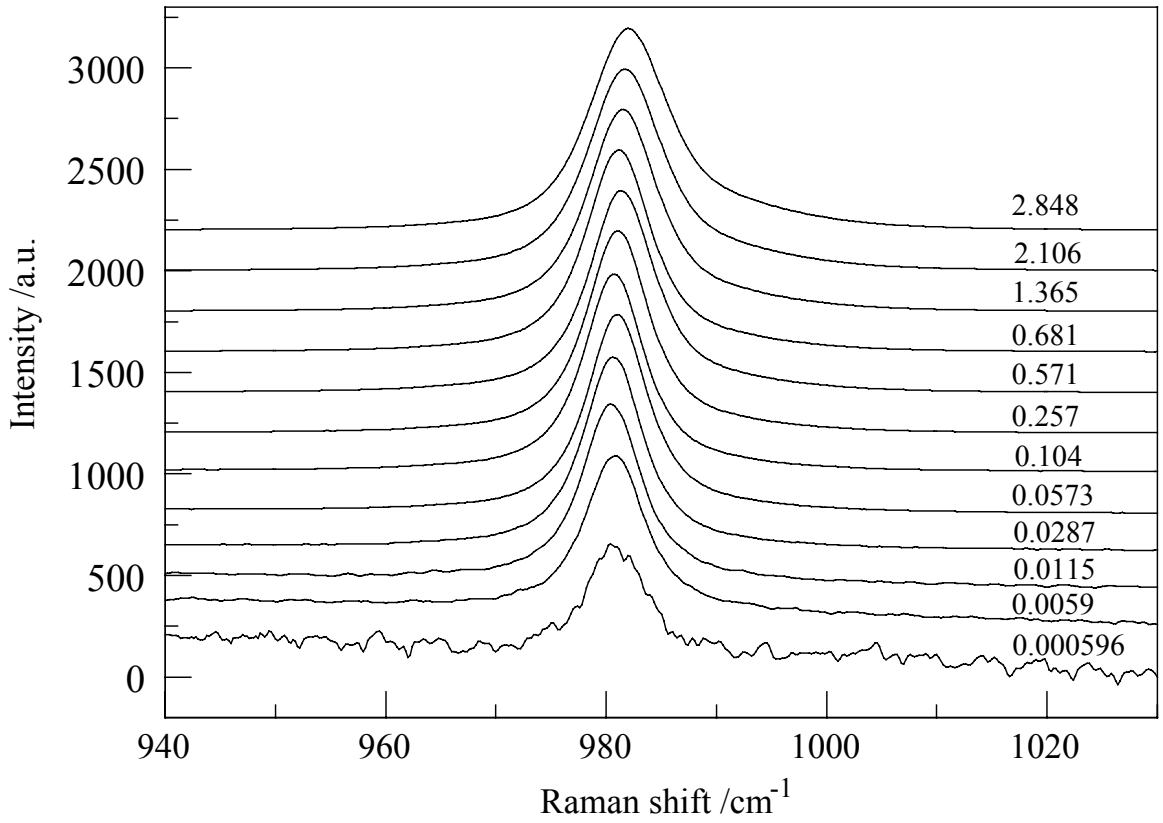
3000
2500
2000
1500
1000
500
0
Intensity /a.u.
940
960
980
1000
1020
Raman shift /cm-1
2.848
2.106
1.365
0.681
0.571
0.257
0.104
0.0573
0.0287
0.0115
0.0059
0.000596

Figure 7

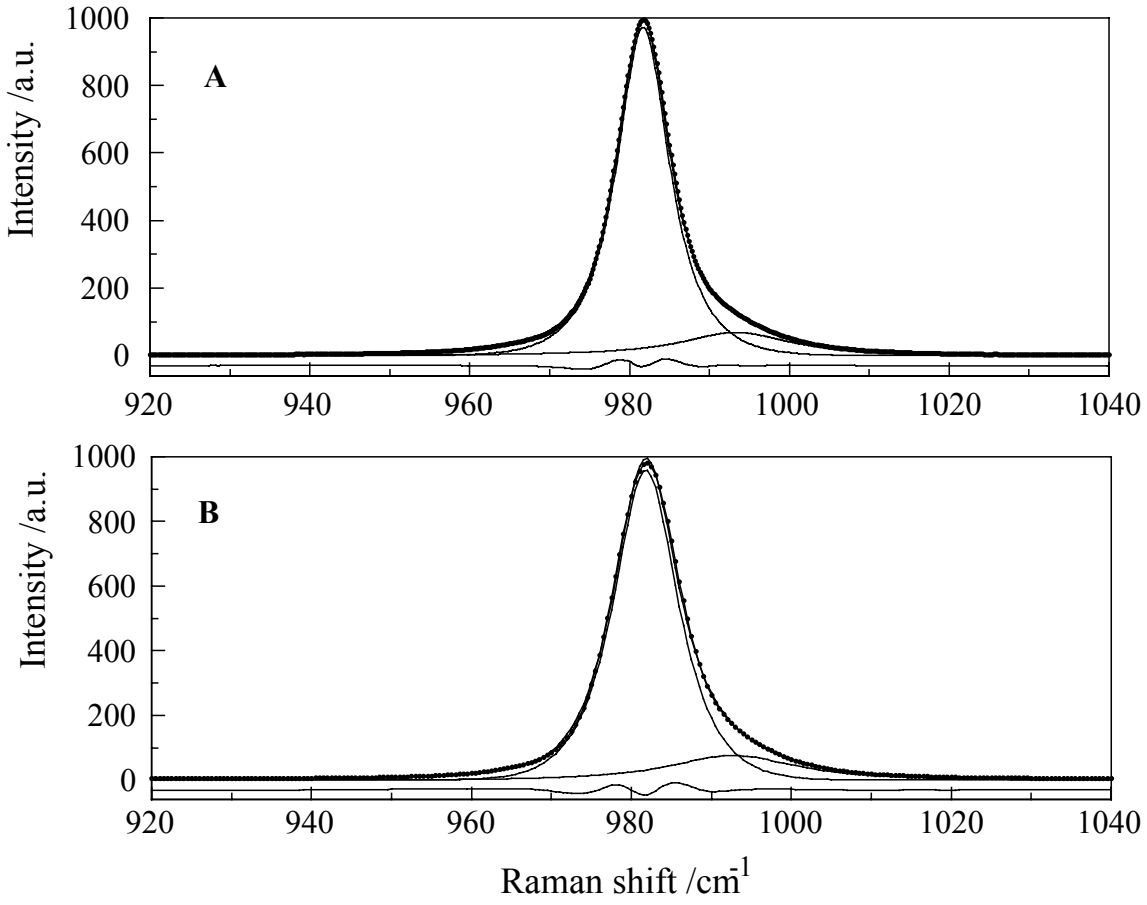
A
B
Intensity /a.u.
Intensity /a.u.
1000
800
600
400
200
0
920
940
960
980
1000
1020
1040
Raman shift /cm-1

Figure 8

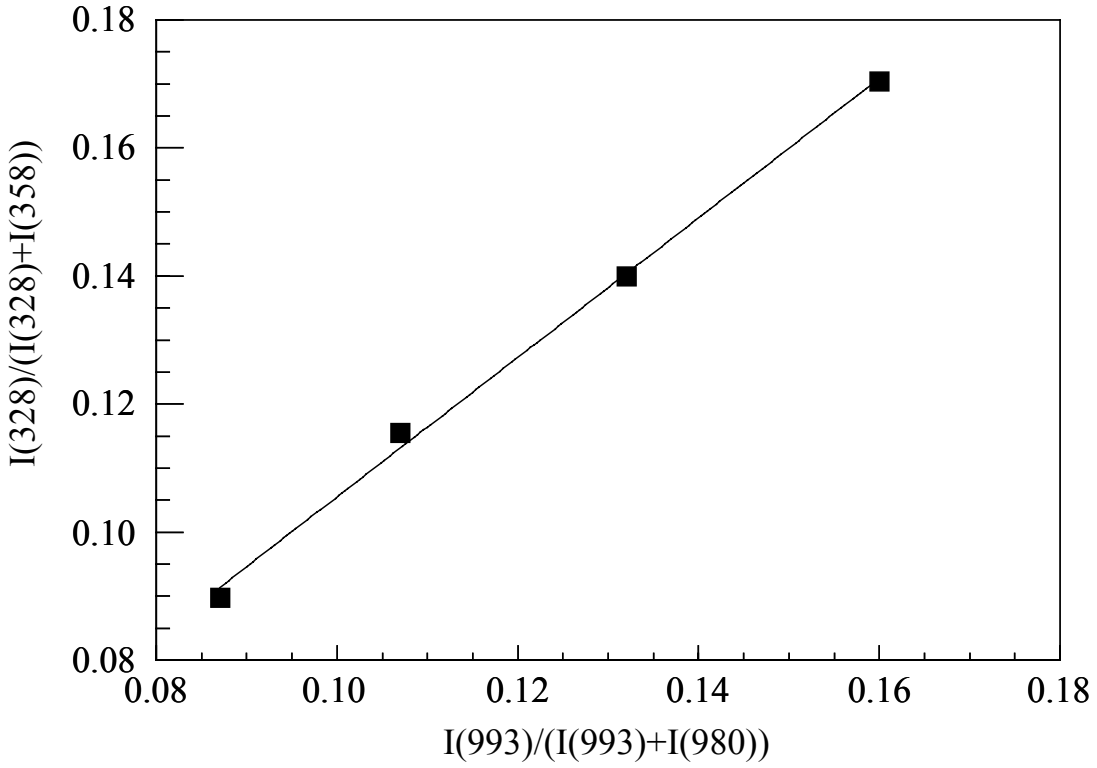
0.18
0.16
0.14
0.12
0.10
0.08
I(328)/(I(328)+I(358))
0.08
0.10
0.12
0.14
0.16
0.18
I(993)/(I(993)+I(980))

Figure 9

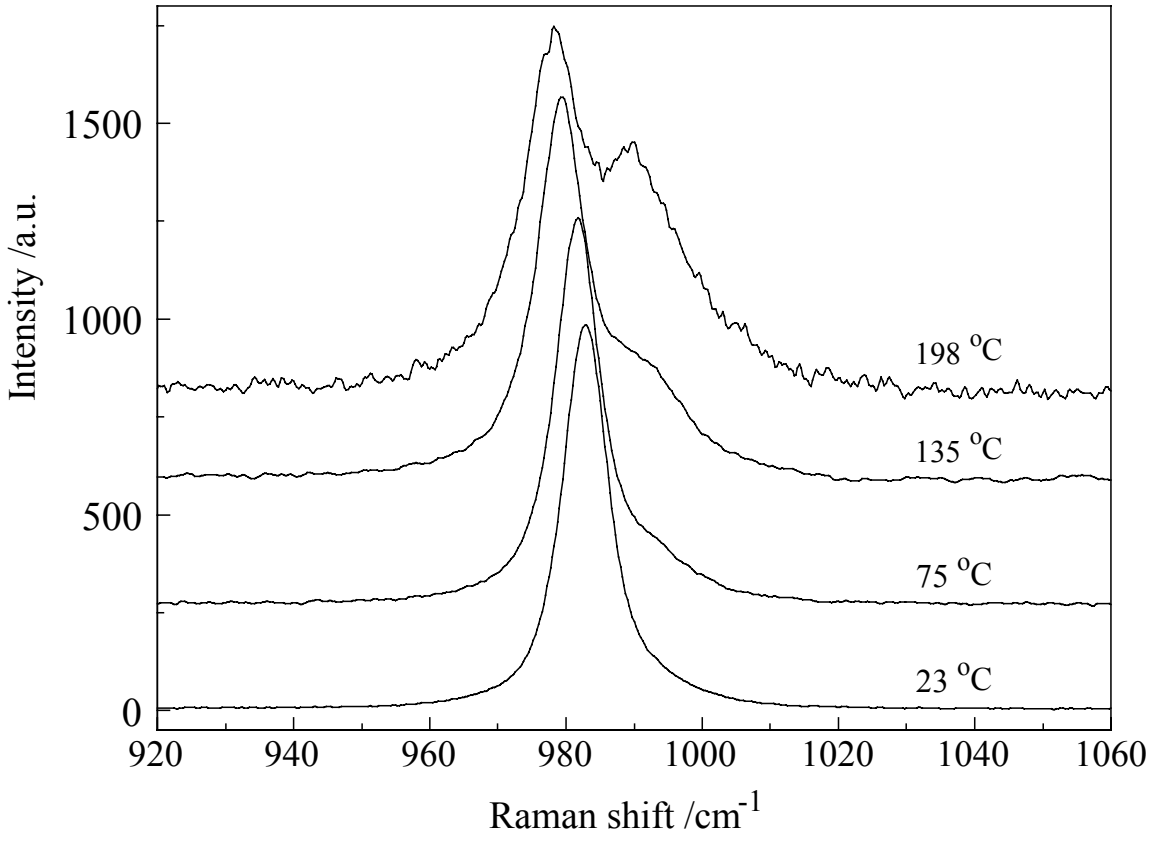
Intensity /a.u.
1500
1000
500
0
920
940
960
980
1000
1020
1040
1060
Raman shift /cm-1
198 oC
135 oC
75 oC
23 oC

Figure 10

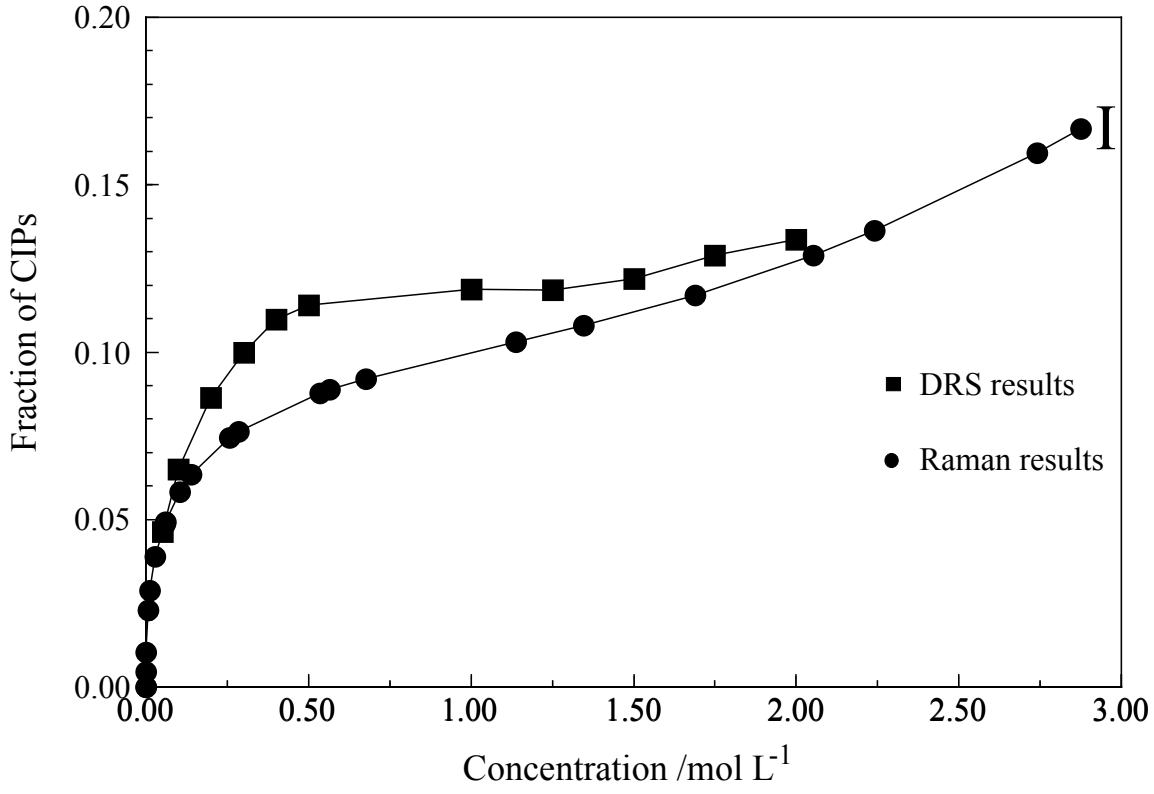
0.20
0.15
0.10
0.05
0.00
Fraction of CIPs
0.00
0.50
1.00
1.50
2.00
2.50
3.00
Concentration /mol L-1
DRS results
Raman results
I

Figure 11

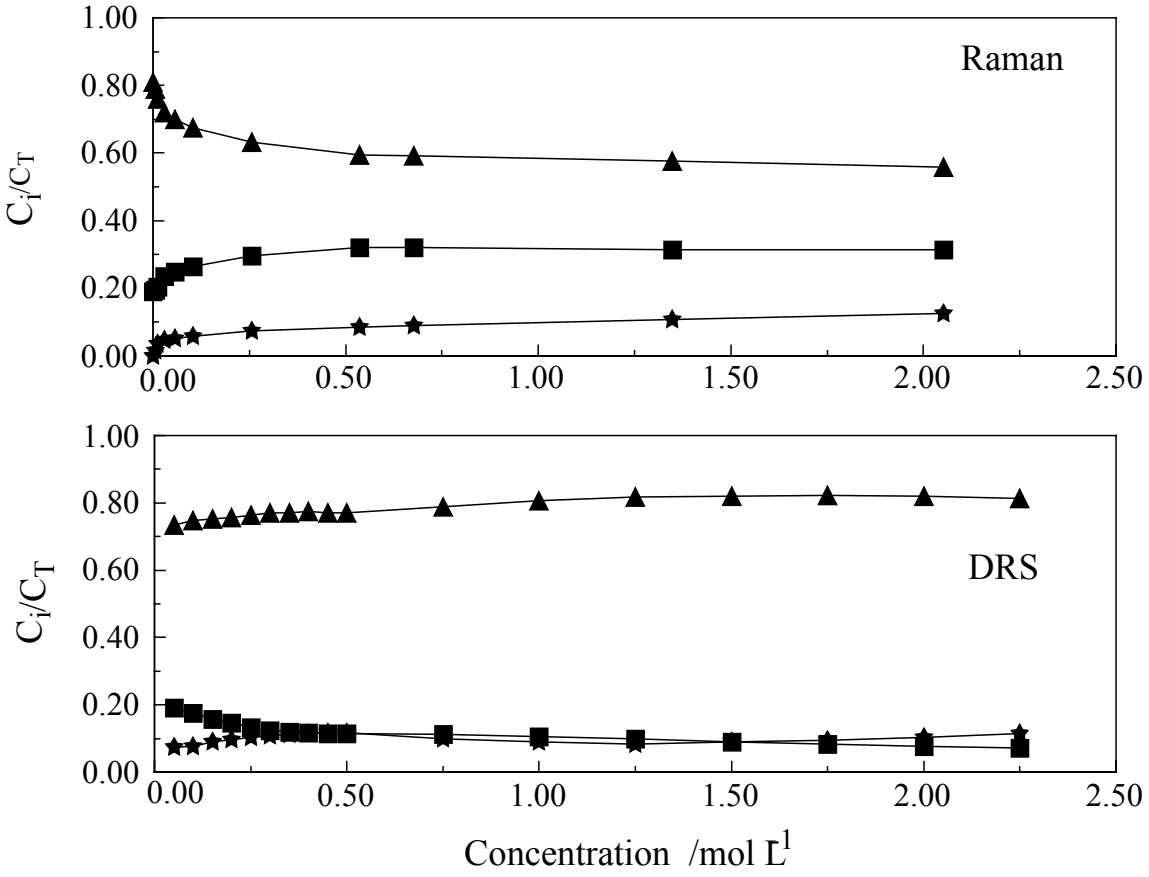
Raman
DRS
C_i/C_T
C_i/C_T
1.00
0.80
0.60
0.40
0.20
0.00
0.00
0.50
1.00
1.50
2.00
2.50
Concentration /mol L^{-1}

Figure 12

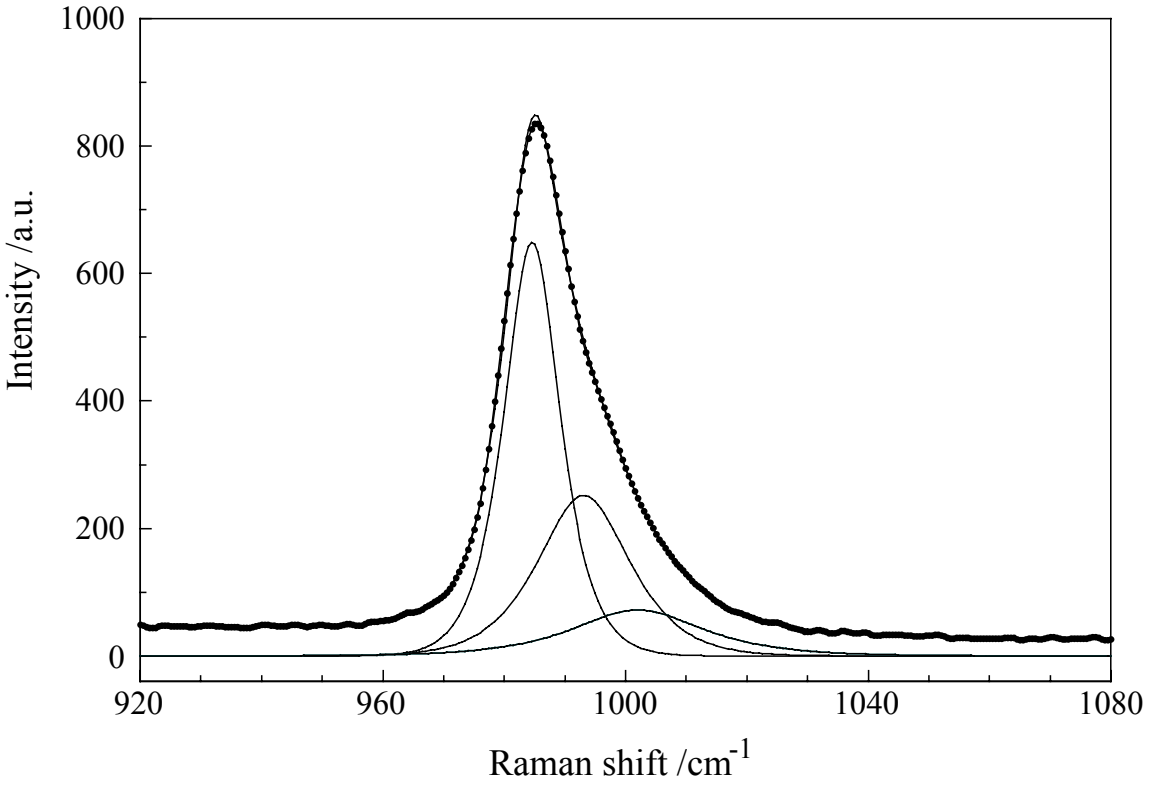
1000
800
600
400
200
0
Intensity /a.u.
920
960
1000
1040
1080
Raman shift /cm-1

Figure 13

Note added at proof: A recent Raman spectroscopic study by Tomišic and Simeon[42] of nominally strong electrolyte solutions, including $MgSO_4$(aq), has come to our attention since submission of this paper. No profiles for the $_{\nu 1}$-$SO4^{-2}$ mode were given[42] but the component peak positions derived by evolving factor analysis (EFA) were stated to be 984 cm^{-1} for 'free' sulfate and 989 cm^{-1} for the CIP. These differ markedly from the present results and those of others.[7,10] Although insufficient detail (such as scattering geometry, spectral resolution, etc.) was presented to allow a proper assessment of the spectra of Tomišic and Simeon,[42] the stated sampling interval of 2 cm^{-1} is probably too large for precise profile analysis by EFA or other common curve fitting techniques. With such smeared-out profiles it is not surprising that their peak locations differ from, and that they were unable to detect the effects observed in, the present study. The suggestion by the authors[42] that EFA had not been used previously in Raman spectral studies of ion association appears to have overlooked the 1977 review by Shurvell and Bulmer.[43]

42 V. Tomišic and V. Simeon, Phys. Chem. Chem. Phys., 2000, 2, 1943.

43 H. F. Shurvell, and J. T. Bulmer, in Vibrational Spectra and Structure, ed. J. R. Durig, Elsevier, Amsterdam, 1977, vol. 6, ch. 2.